Dalton Transactions

ROYAL SOCIETY OF CHEMISTRY

PAPER

View Article Online
View Journal | View Issue

Check for updates

Cite this: *Dalton Trans.*, 2023, **52**, 2098

Diphenylacetylene stabilised alkali-metal nickelates: synthesis, structure and catalytic applications†

Andryj M. Borys and Eva Hevia *

Received 8th January 2023,
Accepted 10th January 2023

DOI: 10.1039/d3dt00069a

rsc.li/dalton

Whilst low-valent nickelates have recently been proposed as intermediates in Ni-catalysed reactions involving polar organometallics, their isolation and characterisation is often challenging due to their high sensitivity and reactivity. Advancing the synthetic, spectroscopic and structural insights of these heterobimetallic systems, here we report a new family of alkyne supported alkali-metal nickelates of the formula $Li_4(solv)_n(Ar)_4Ni_2\{\mu_2{:}\eta^2,\eta^2\text{-Ph–C}\equiv\text{C–Ph}\}$ (where solv = Et_2O, THF; Ar = Ph, *o*-Tol, naphthyl, 4-^{t}Bu-C_6H_4) which can be accessed through the combination of $Ni(COD)_2$, Ph–C≡C–Ph and the relevant lithium aryl in a 2 : 1 : 4 ratio. Demonstrating the versatility of this approach, the sodium and potassium nickelates can also be accessed when using PhNa or *via* alkali-metal exchange with AMO^tBu (AM = Na, K). When employing bulky or structurally constrained aryl-lithiums, mononickel complexes of the formula $Li_2(solv)_n(Ar)_2Ni\{\eta^2\text{-Ph–C}\equiv\text{C–Ph}\}$ are instead obtained, highlighting the structural diversity of alkali-metal nickelates bearing alkyne ligands. Expanding the catalytic potential of these systems, their ability to promote the catalytic cyclotrimerisation of diphenylacetylene to hexaphenylbenzene was explored, with mononickel compounds bearing electron rich aryl-substituents displaying the best performance.

Introduction

The coordination of polar organometallics to Ni(0) was first investigated in the early 1970s,[1,2] and succeeded the pioneering work of Wilke into ubiquitous Ni(0)-olefin complexes such as $Ni(C_2H_4)_3$,[3] Ni(*ttt*-CDT)[4] and $Ni(COD)_2$.[5] It was observed that the treatment of these Lewis acidic Ni(0) complexes with simple polar organometallics can give rise to highly sensitive anionic nickelates in which the formally carbanionic centre now coordinates to Ni(0), often with displacement of an olefin ligand.[2] Several examples of anionic nickelates were documented during these early studies, with a range of polar organometallics such as organolithiums,[6–10] organomagnesiums,[11] organoaluminium[12] or hydrido-aluminate species.[13–15] Typically, one or more olefins remain coordinated to Ni(0) to act as a π-accepting ligand to modulate the high electron density at the d^{10} metal centre.[2] In the absence of olefins, through forced displacement with excess PhLi or PhNa, it was discovered that even N_2 can coordinate in a side-on and bridging motif $\{\mu_2\text{-}\eta^2{:}\eta^2\}$ between two Ni centres,[16–18] hinting at the key role of π-accepting ligands for the stabilisation and isolation of low valent nickelates. For alkali-metal nickelates, examples of both charge-separated (Scheme 1a, **I**)[6,9] and contacted ion-pair species (Scheme 1a, **II** and **III**)[19,20] are known, with alkali-metal : nickel ratios ranging from 1 : 1, 2 : 1 or 3 : 1.

Despite exhibiting a wealth of unique structural features, low-valent anionic nickelates remained dormant in the literature for several decades and were overshadowed by parallel developments on the applications of nickel complexes in catalysis.[21] More recently, however, it has been proposed by theoretical studies that low-valent nickelates may be potential intermediates in certain nickel-catalysed cross-coupling reactions involving polar organometallics,[22,23] prompting a renewed experimental interest into these overlooked species.

We have previously explored the rich co-complexation chemistry of $Ni(COD)_2$ and PhLi, which gives a series of lithium nickelates including **II** (Scheme 1), and demonstrated that these are key intermediates in the nickel-catalysed cross-coupling of aryl ethers.[19,24] When further assessing these co-complexation reactions, we found that using a larger excess of PhLi led to the formation of a polynuclear dinickel cluster containing a bridging C_6H_4 dianion as a result of intramolecular C–H activation of a phenyl substituent (Scheme 1, **IV**).[25] The formation of **IV** suggests that the homoleptic tri-lithium nickelate "$Li_3NiPh_3(solv)_3$" is too electron-rich to form, leading to the *in situ* formation of the π-accepting benzyne-type ligand. Only when moving to organolithiums which themselves could serve as π-accepting ligands, namely lithium aryl acetylides, is it possible to isolate homoleptic tri-lithium nickelates **III**,

Departement für Chemie, Biochemie und Pharmazie, Universität Bern, 3012 Bern, Switzerland. E-mail: eva.hevia@unibe.ch

†Electronic supplementary information (ESI) available: Full synthetic details, crystallographic information, and NMR spectra. CCDC 2221333–2221339. For ESI and crystallographic data in CIF or other electronic format see DOI: https://doi.org/10.1039/d3dt00069a

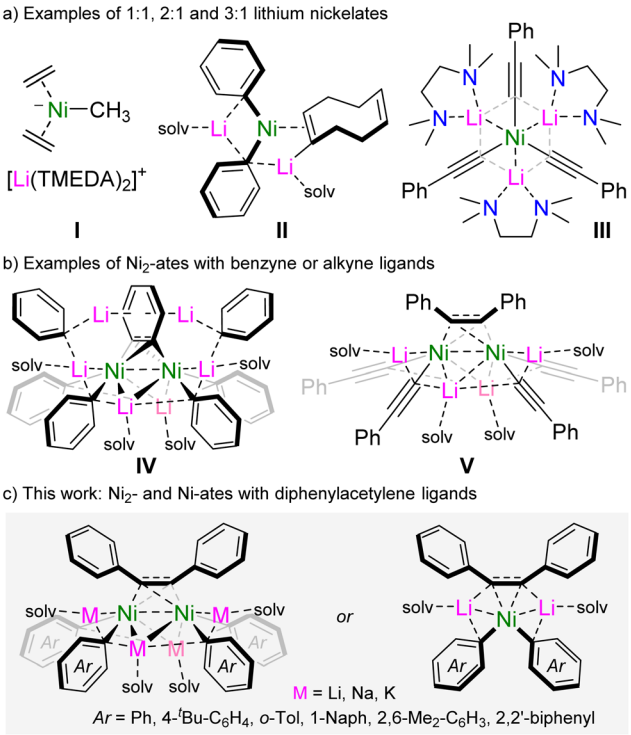

Scheme 1 Selected examples of alkali-metal nickelates.

which were found to be further stabilised by London dispersion interactions.[20] Notably, compound **III** reacts with PhI to give **V** in which the cross-coupled product (diphenylacetylene) is trapped and coordinated in a bridging motif between two nickel centres. Since **V** bears similar structural features to **IV**, we thus considered whether it was possible to use diphenylacetylene as a simple π-accepting ligand to access new families of alkali-metal nickelates. Herein, we detail synthetic and structural insights into dinickel and mononickelate complexes which can be readily accessed by reacting $Ni(COD)_2$ with two molar equivalents of alkali-metal aryls in the presence of diphenylacetylene. Advancing the structure/reactivity correlations, we also assess the catalytic ability of these novel heterobimetallic complexes to promote the cyclotrimerisation of diphenylacetylene, as well as its insertion into biphenylene.

Results and discussion

Synthesis of alkali-metal nickelates

The reported dinickel complex $[(COD)Ni]_2\{\mu_2\text{-}\eta^2\text{:}\eta^2\text{-Ph–C}\equiv\text{C–Ph}\}$ was selected as a suitable precursor to target alkali-metal dinickelates.[26,27] Addition of PhLi (2 equivalents per Ni) to an Et_2O solution of *in situ* prepared $[(COD)Ni]_2\{\mu_2\text{-}\eta^2\text{:}\eta^2\text{-Ph–C}\equiv\text{C–Ph}\}$ gave the corresponding hexanuclear lithium nickelate, $Li_4(Et_2O)_4Ph_4Ni_2\{\mu_2\text{-}\eta^2\text{:}\eta^2\text{-Ph–C}\equiv\text{C–Ph}\}$ (**1a**), as a dark red crystalline solid in 41% yield (Scheme 2). The formation of dinickelate complex **1a** contrasts with the mononickel complex $Li_2(THF)_4Ph_2Ni(COD)$ (**II**, Scheme 1a) which is prepared from $Ni(COD)_2$ and 2 equivalents of PhLi,[19] reflecting the differing coordination ability of alkyne ligands in comparison to traditionally employed olefin ligands. This procedure could be

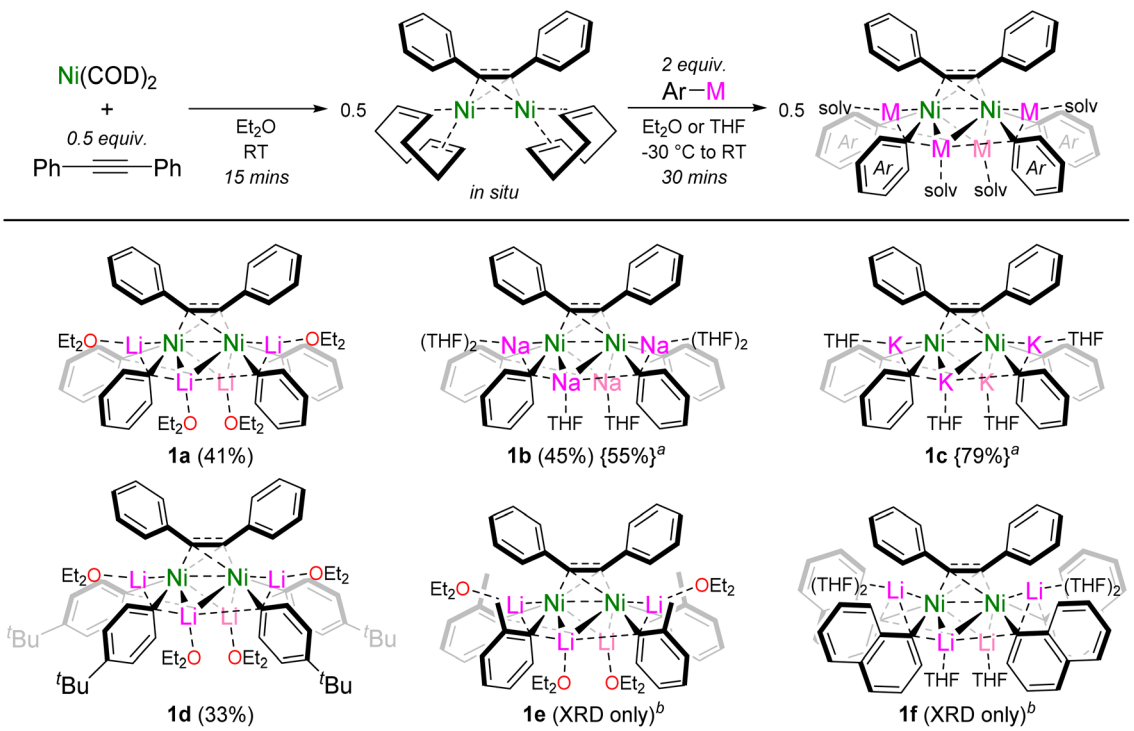

Scheme 2 Synthesis of dinickelate complexes **1a–f**. Isolated crystalline yields given in parentheses. [a] Prepared by treating **1a** with NaO^tBu or KO^tBu, respectively. [b] Could not be isolated in pure form.

extended to PhNa to give the analogous sodium nickelate, $Na_4(THF)_6Ph_4Ni_2\{\mu_2\text{-}\eta^2\text{:}\eta^2\text{-Ph–C}\equiv\text{C–Ph}\}$ (**1b**), but attempts to prepare the potassium nickelate directly from PhK failed however, likely due to competing side reactions of PhK with the ethereal solvent or 1,5-cyclooctadiene.[25] Alkali-metal exchange through the treatment of **1a** with 4 equivalents of KO^{t}Bu proved successful nevertheless, to give the corresponding potassium nickelate, $K_4(THF)_4Ph_4Ni_2\{\mu_2\text{-}\eta^2\text{:}\eta^2\text{-Ph–C}\equiv\text{C–Ph}\}$ (**1c**) in 79% yield. This represents the first homologous series of alkali-metal nickelates bearing different alkali-metals. Substituted aryl-lithiums such as 4-^{t}Bu-C_6H_4–Li were also compatible to give $Li_4(Et_2O)_4(4\text{-}^t\text{Bu-C}_6H_4)_4Ni_2\{\mu_2\text{-}\eta^2\text{:}\eta^2\text{-Ph–C}\equiv\text{C–Ph}\}$ (**1d**). When using *o*-Tol-Li or 1-naphthyl-Li, the corresponding hexanuclear lithium nickelates $Li_4(Et_2O)_4(o\text{-Tol})_4Ni_2\{\mu_2\text{-}\eta^2\text{:}\eta^2\text{-Ph–C}\equiv\text{C–Ph}\}$ (**1e**) and $Li_4(THF)_6(1\text{-Naph})_4Ni_2\{\mu_2\text{-}\eta^2\text{:}\eta^2\text{-Ph–C}\equiv\text{C–Ph}\}$ (**1f**) could be structurally characterised by single-crystal X-ray diffraction, but could not be isolated in pure form (*vide infra*). Whilst the treatment of $[(COD)Ni]_2\{\mu_2\text{-}\eta^2\text{:}\eta^2\text{-Ph–C}\equiv\text{C–Ph}\}$ with aryl-lithiums appeared to be selective and quantitative by NMR spectroscopy (see Fig. S1†), isolated crystalline yields of the alkali-metal nickelates were typically low (33–45%) due to their high solubility in ethereal solvents.

Interestingly, we also found that by systematically studying these co-complexation reactions when using *ortho*-substituted aryl-lithiums, *o*-Tol-Li and 1-naphthyl-Li, the formation of mononickelate complexes of the formula $Li_2(solv)_n(Ar)_2Ni\{\eta^2\text{-Ph–C}\equiv\text{C–Ph}\}$ was instead favoured, with the choice of donor solvent playing an important role in dictating the crystallised product. With *o*-Tol-Li, small quantities of the Et_2O solvate (**1e**) could be crystallised, but samples were always plagued with variable amounts $Ni(COD)_2$ or $[(COD)Ni]_2\{\mu_2\text{-}\eta^2\text{:}\eta^2\text{-Ph–C}\equiv\text{C–Ph}\}$, preventing its isolation in pure form. Contrastingly, performing the reaction with one equivalent of diphenylacetylene in the presence of THF, allowed $Li_2(THF)_2(o\text{-Tol})_2Ni\{\eta^2\text{-Ph–C}\equiv\text{C–Ph}\}$ (**2a**) to be reliably prepared and isolated in pure form (Scheme 3). Similarly with 1-naphthyl-Li, small quantities of the THF solvate (**1f**) could be crystallised, but not isolated in pure form. Performing the reaction with one equivalent of diphenylacetylene in Et_2O however, allowed for the reliable isolation of $Li_2(Et_2O)_2(1\text{-Naph})_2Ni\{\eta^2\text{-Ph–C}\equiv\text{C–Ph}\}$ (**2b**). Further exploring how general the formation of mononickelate alkyne complexes was, the bulky aryl-lithium 2,6-Me_2-C_6H_3-Li also gave $Li_2(Et_2O)_2(2,6\text{-Me}_2\text{-C}_6H_3)_2Ni\{\eta^2\text{-Ph–C}\equiv\text{C–Ph}\}$ (**2c**), whilst the structurally constrained aryl-lithium, 2,2′-dilithiobiphenyl, reacted smoothly to give $Li_2(THF)_4(2,2'\text{-biphenyl})Ni\{\eta^2\text{-Ph–C}\equiv\text{C–Ph}\}$ (**2d**). Compound **2d** is closely related to the dilithionickelole $Li_2(THF)_4(2,2'\text{-biphenyl})Ni\{\eta^2,\eta^2\text{-COD}\}$ which was previously reported by Xi and co-workers.[28]

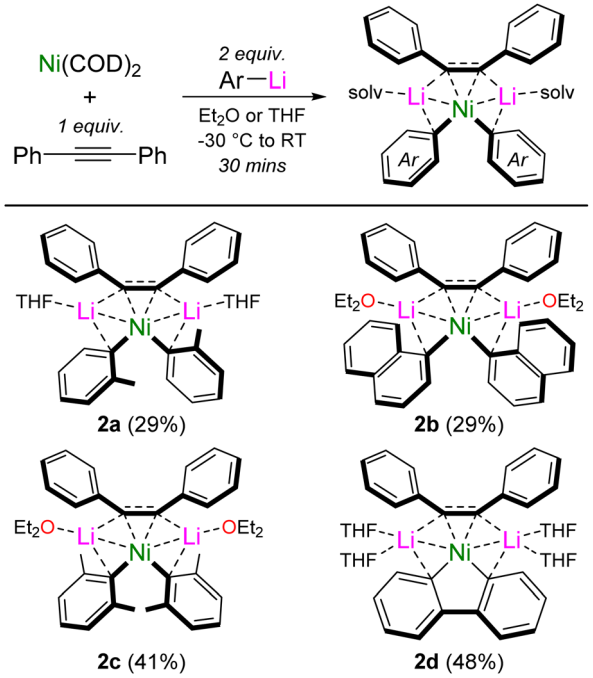

Scheme 3 Synthesis of mononickelate complexes **2a–d**. Isolated crystalline yields given in parentheses.

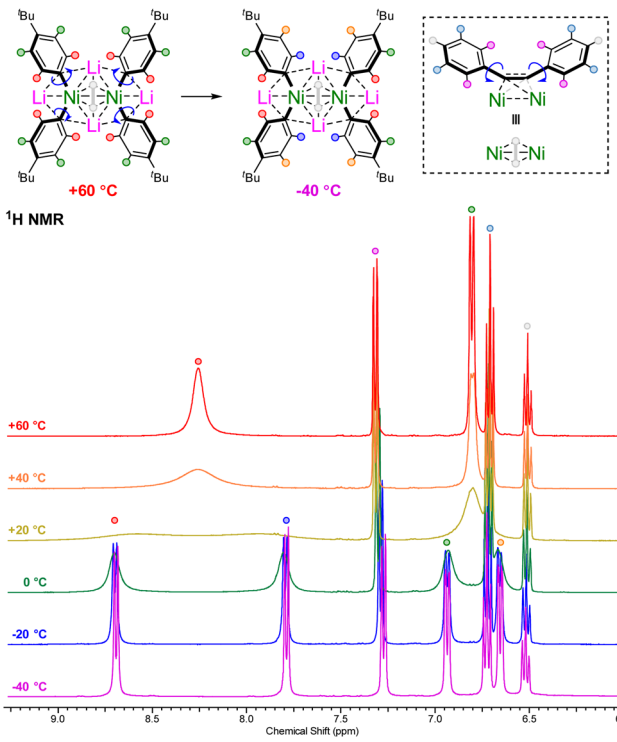

Fig. 1 Variable temperature ^{1}H NMR spectra of **1d** in THF-d_8 illustrating fast or frozen rotation about the C_{aryl}–Ni bonds.

Spectroscopic features

The alkali-metal nickelates **1a–d** and **2a–d** typically show sharp and well resolved ^{1}H, ^{7}Li and ^{13}C NMR spectra, consistent with d^{10} diamagnetic Ni(0) species. Contrastingly, compound **1d** displayed broad signals in the room temperature ^{1}H NMR spectrum for the coordinated 4-^{t}Bu-C_6H_4-substituents (Fig. 1, yellow trace), alongside two broad ^{7}Li NMR resonances at δ 0.26 and −0.59 (ESI, Fig. S3†). Cooling to −40 °C (Fig. 1, purple trace) leads to splitting of the broad *ortho* and *meta*-proton signals

into two distinct and well-resolved resonances for each, consistent with frozen rotation about the C_{aryl}–Ni bonds. Heating to +60 °C (Fig. 1, red trace) on the other hand, leads to coalescence of the signals in both the ^{1}H and ^{7}Li NMR spectra, indicative of fast rotation about the C_{aryl}–Ni bonds on the NMR timescale. These spectroscopic observations suggest that the electron-rich 4-^{t}Bu-C_6H_4-substituent coordinates stronger to nickel in comparison to other aryl-substituents.

The di- and mono-nickelate complexes can be further distinguished by assessing the $^{13}C\{^{1}H\}$ NMR signal of the acetylene carbon. For compounds **1a–d**, this signal is observed in the range of δ 68.6–76.6, which is considerably shielded compared to [(COD)Ni]$_2$\{μ_2-η^2:η^2-Ph–C≡C–Ph\} (δ 106.9), and consistent with significant back-donation from the electron-rich Ni centres. Contrastingly, the acetylene carbon signal for compounds **2a–d** is observed in the range δ 144.9–150.8, which is considerably deshielded compared to free diphenylacetylene (δ 90.8),[29] and slightly shielded when compared to other L_2Ni\{η^2-Ph–C≡C–Ph\} complexes [L = N-heterocyclic carbene (δ 139.3)[30] or diphosphine (δ 141.3)].[31] The C_{aryl}–Ni *ipso*-carbon signal for compounds **1a**, **1d** and **2a–d** is observed in the range δ 177.2–191.1, which is similar to other phenyl-nickelate complexes such as **II** and **IV** (Scheme 1),[19,25] and comparable to the free aryl-lithiums (see ESI† for full spectroscopic details). Notably, the *ipso*-carbon signal for the phenyl-derivatives becomes more deshielded on moving from Li (**1a**; δ 182.0) to Na (**1b**; δ 195.8) to K (**1c**; δ 203.8), consistent with increased charge density at the carbanionic centre.[32]

Solid-state structures

Single crystals suitable for X-ray diffraction studies were obtained for dinickelate complexes **1a–b** and **1d–f**, and selected crystallographic parameters are shown in Table 1 (see ESI† for further details and full structures). Whilst single crystals of potassium nickelate **1c** could be grown, they were found to immediately desolvate and lose crystallinity when removed from the mother liquor, a feature we have previously observed for other alkali-metal nickelates.[33] The Ni–C_{aryl} distances are comparable for compounds **1a–b** and **1d–f** and range from 1.952(2)–2.042(8) Å, which is similar to previously reported nickelates derived from PhLi or PhNa.[7,8,16–19,25] The Ni···M (M = Li, Na) distances are close to or longer than the sum of covalent radii,[34] with increasing distances as the size of the alkali-metal cation increases down group 1. Previous complementary bonding analysis on **III** (Scheme 1) revealed that there is no direct Ni···M bonding,[20] and therefore there is likely no bonding interaction between nickel and the alkali-metal cations in compounds **1a–f**. Similarly, the Ni···Ni distances [range = 2.633(3)–2.8873(7) Å] are longer than observed for reported Ni–Ni bonds (*ca.* 2.3–2.5 Å),[35] and comparable to **IV** in which no Ni–Ni bond was found from natural bond order (NBO) analysis.[25] The C≡C (C6–C7) distance of the co-ordinated diphenylacetylene ranges from 1.38(2)–1.394(2) Å; this is significantly longer than free diphenylacetylene [1.198(2) Å][36] and consistent with considerable back-donation from the electron-rich Ni centres. In addition, the coordinated diphenylacetylene shows considerable bending away from linearity [C5–C6–C7 or C8–C7–C6; 125.2(9)–132.6(1)°].

A close inspection into the structures of compounds **1e** and **1f**, which are derived from *o*-Tol-Li and 1-naphthyl-Li respectively, reveal considerable structural distortion when compared to lithium nickelates **1a** and **1d**. In the solid-state structure of **1e**, all *ortho*-CH_3 substituents are orientated in the same direction towards the coordinated diphenylacetylene unit with Ni–C_{aryl}–C_{ortho}–CH_3 torsion angles ranging from 1.5(3)–6.4(3)° (Fig. 2 & Fig. S10†). Most notably, one of the four Et_2O molecules coordinates to Li2 *via* anagostic interactions (*i.e.* largely electrostatic) from the CH_3 group [C–H···Li2 = 2.817–3.189 Å], in contrast to the expected oxygen coordination mode observed for Li1, Li3 and Li4. This is likely a consequence of the shorter Li2···C2 and Li2···C3 distances [2.257(4) Å and 2.197(4) Å, respectively] when compared to the Li3···C1 and

Table 1 Selected crystallographic parameters for compounds **1a–b** and **1d–f**

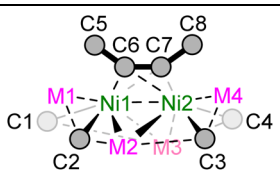

	Distance/Å								Angle/°		Torsion/°
Compound	Ni1–C1	Ni–C2	Ni2–C3	Ni2–C4	Ni···M range	Ni1···Ni2	Ni–C6/7 range	C6–C7	C5–C6–C7	C8–C7–C6	C5–C6–C7–C8
1a	1.986(2)	1.965(1)	1.986(2)	1.965(1)	2.469(3)–2.663(3)	2.633(3)	1.947(1)–1.968(1)	1.394(2)	127.6(1)	127.6(1)	5.0(2)
	1.980(1)	1.977(2)	1.980(1)	1.977(2)	2.441(1)–2.654(3)	2.654(3)	1.936(1)–1.979(1)	1.388(2)	127.6(1)	127.6(1)	5.8(2)
1b	2.042(8)	1.957(3)	2.042(8)	1.957(3)	2.825(1)–3.099(1)	2.8873(7)	—[a]	1.38(2)	125.2(9)	125.2(9)	—[a]
1d	1.980(2)	1.983(2)	1.973(2)	1.968(2)	2.395(5)–2.628(4)	2.7079(8)	1.948(2)–1.964(2)	1.392(3)	127.7(2)	127.5(2)	3.0(4)
1e	1.958(2)	1.952(2)	1.987(2)	1.965(2)	2.448(3)–2.758(3)	2.7906(7)	1.921(1)–2.013(2)	1.386(2)	132.6(1)	129.8(1)	20.1(3)
1f	1.977(3)	1.959(3)	1.977(3)	1.959(3)	2.674(5)–2.770(5)	2.8218(8)	1.931(3)–2.027(3)	1.381(3)	127.2(2)	127.2(2)	14.8(4)
	1.953(3)	1.975(4)	1.953(3)	1.975(4)	2.587(6)–2.795(6)	2.7606(6)	1.925(3)–2.034(2)	1.392(4)	126.7(2)	126.7(2)	21.8(4)

[a] The Ph–C≡C–Ph is disordered across two positions.

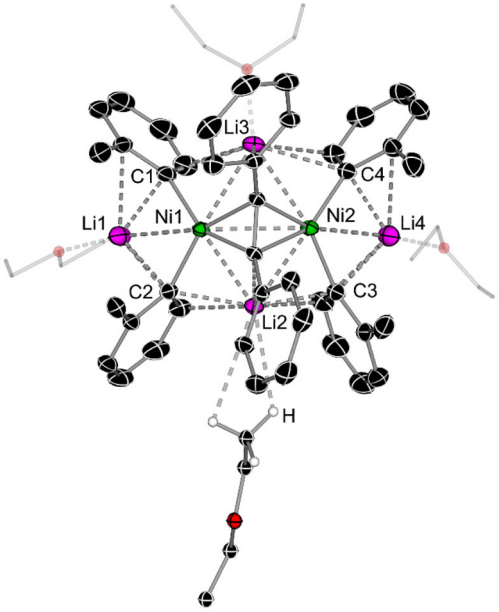

Fig. 2 Molecular structure of **1e**. Thermal ellipsoids shown at 30% probability and hydrogen atoms (except those on Et_2O showing anagostic interactions to Li2) omitted for clarity. See Fig. S10† for alternative view.

Li3···C4 distances [2.446(4) Å and 2.563(3) Å, respectively]. Anagostic interactions between CH_3 groups and Li have been observed in several crystal structures,[37,38] including in lithium nickelates,[39] but this is limited to intramolecular examples. In addition, there is considerable torsion in the diphenylacetylene unit [C5–C6–C7–C8 = 20.1(3)°, see Table 1 for general label numbering] to enable additional C_{arene}···Li2 interactions [2.727(4)–2.750(4) Å].

In the solid-state structure of **1f** (see Fig. S11† for full structure), the 1-naphthyl substituents are similarly all orientated in the same direction towards the coordinated diphenylacetylene unit with Ni–C_{aryl}–C_{ortho}–CH_3 torsion angles ranging from 2.9(5)–5.4(5)°. As with **1e**, there is also significant torsion in the coordinated diphenylacetylene unit [C5–C6–C7–C8 = 14.8(4)° or 21.8(4)°] to enable additional C_{arene}···Li2/3 interactions [2.671(5)–2.998(6) Å]. The central core of **1f** shows considerable distortion when compared to **1a** (Fig. 3). For example, in **1a**, the four *ipso*-carbons (C1–C4) lie in an approximate plane which sits co-planar below the mean plane of all four lithium atoms (Li1–Li4). In **1f**, neither the four *ipso*-carbons (C1–C4) or the four Li atoms (Li1–Li4) reside in an approximate plane. Whilst Li2 and Li3 are approximately co-planar with Ni1 and Ni2 (~0.1 Å deviation), Li1 and Li4 sit considerably lower than Li2/Li3 and Ni1/Ni2, as well as the four *ipso*-carbons (C1–C4). This exposes the Li1/Li4 cations such that two molecules of THF can coordinate to each lithium, in contrast to only one molecule of coordinated Et_2O observed in **1a**, **1d** and **1e**. Whilst the identity of the ethereal solvent clearly impacts the isolation and crystallisation of compounds **1e** and **1f** over their mononickelate analogues **2a** and **2b**, it is unclear whether the

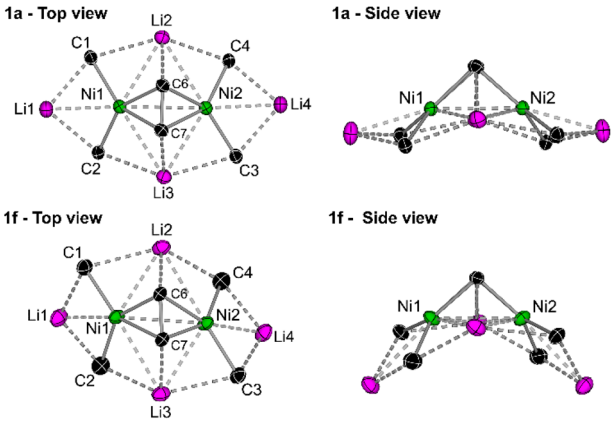

Fig. 3 Simplified top and side views of the hexanuclear cores of **1a** and **1f** illustrating the structural distortion in **1f** when compared to **1a**.

unique solvent coordination in **1e** and **1f** is the cause or simply a consequence of the observed structural distortions.

In the solid-state structure of mononickelate complexes **2c** and **2d** (Fig. 4), the Ni centre adopts a pseudo trigonal planar geometry in which the diphenylacetylene coordinates in a η^2-fashion. The Ni···C≡C distances are shorter [1.892(1)–1.932(1) Å for **2c**; 1.877(2)–1.881(2) Å for **2d**] when compared to dinickelate complexes **1a–f** (see Table 1). In addition, the C≡C bond lengths [1.318(2) Å for **2c**; 1.324(2) for **2d**] are shorter, and the C_{ipso}–C≡C angles are closer to 180° [134.8(1)–135.4(1)° for **2c**; 136.1(1)–137.6(1)° for **2d**], indicative of weaker overall backbonding from Ni to the coordinated diphenylacetylene. The Li···Ni distances for **2c** and **2d** range from 2.408(3)–2.515(3) Å, which is comparable to dinickelate complexes **1a** and **1d–f**, and other structurally characterised lithium nickelates.[19,20,25]

Catalytic cyclotrimerisation of diphenylacetylene

The unique coordination modes of diphenylacetylene observed in alkali-metal nickelates **1a–d** and **2a–d**, and significant backdonation prompted us to assess their catalytic activity in the cyclotrimerisation of diphenylacetylene. Numerous transition-metal complexes have been reported to catalyse the [2 + 2 + 2]

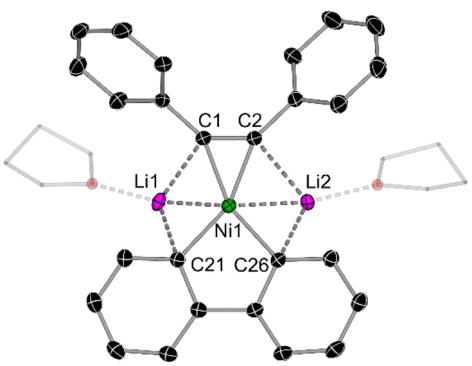

Fig. 4 Molecular structure of **2d**. Thermal ellipsoids shown at 30% probability. Hydrogen atoms and two molecules of coordinated THF omitted for clarity.

cyclotrimerisation of alkynes to give poly-substituted benzene derivatives.[40–42] Following on from the pioneering work of Reppe into the nickel catalysed oligomerisation of acetylene,[43–45] several nickel complexes have now been developed for the catalytic oligomerisation or cycloaddition of substituted alkynes and related substrates.[46,47] Selected examples include work by Guan which showed that $Ni(COD)_2/PPh_3$ is a simple but highly efficient catalyst for the cyclotrimerisation of terminal and internal alkynes.[48] Uyeda has employed chelating diamine ligands to assess how metal nuclearity (*i.e.* mono-nickel *vs.* dinickel) impacts the activity and selectivity of alkyne oligomerisation.[49]

The catalytic activity of the neutral dinickel olefin complexes $[(COD)Ni]_2\{\mu_2\text{-}\eta^2\text{:}\eta^2\text{-Ph–C}\equiv\text{C–Ph}\}$[27] and Ni_2COT_2 (COT = cyclooctatetraene)[50] was first evaluated (Table 2 and Table S1†). Using 5 mol% of dinickel catalyst, only modest conversions (38% and 41%, respectively) of diphenylacetylene was observed after heating to 80 °C for 4 hours (entries 1 and 2). Moving to the lithium nickelate $Li_4(Et_2O)_4Ph_4Ni_2\{\mu_2\text{-}\eta^2\text{:}\eta^2\text{-Ph–C}\equiv\text{C–Ph}\}$ (**1a**, entry 3) led to a considerable increase to 74% conversion. Contrasting with other catalytic studies using alkali-metal magnesiates,[51–55] no apparent alkali-metal effect was observed, with comparable conversions observed for the sodium nickelate **1b** (73%, entry 4) and potassium nickelate **1c** (78%, entry 5), indicating that the alkali-metal does not appear to play an active role in catalysis. Using compound **1d** as a catalyst gave a slightly improved conversion (85%, entry 6) suggesting that the more electron-rich 4-^{t}Bu-C_6H_4 substituents enhances the catalytic activity when compared to **1a**. Supporting this claim, the acetylide substituted dinickel compound $Li_4(Et_2O)_4(Ph\text{–}C\equiv C)_4Ni_2\{\mu_2\text{-}\eta^2\text{:}\eta^2\text{-Ph–C}\equiv\text{C–Ph}\}$ (**V**, Scheme 1) was completely inactive for the catalytic cyclotrimerisation of diphenylacetylene (entry 7), but could catalyse the cyclotrimerisation of more activated terminal alkynes such as phenylacetylene (see ESI† for further details).

Full conversion (>95%) of diphenylacetylene was observed when using $Li_2(THF)_2(o\text{-Tol})_2Ni\{\mu_2\text{-}\eta^2\text{:}\eta^2\text{-Ph–C}\equiv\text{C–Ph}\}$ (**2a**, entry 8) or $Li_2(Et_2O)_2(2,6\text{-}Me_2\text{-}C_6H_3)_2Ni\{\mu_2\text{-}\eta^2\text{:}\eta^2\text{-Ph–C}\equiv\text{C–Ph}\}$ (**2c**, entry 10) as the catalyst, demonstrating that the mononickelate complexes show superior catalytic activity compared to the dinickelate complexes **1a–d**. The electron-deficient derivative $Li_2(Et_2O)_2(1\text{-Naph})_2Ni\{\mu_2\text{-}\eta^2\text{:}\eta^2\text{-Ph–C}\equiv\text{C–Ph}\}$ (**2b**) showed reduced conversions (74%, entry 9), again illustrating how the electronic properties of the aryl-substituents can influence catalytic activity.

Interestingly, when using $Li_2(THF)_4(2,2'\text{-biphenyl})Ni\{\mu_2\text{-}\eta^2\text{:}\eta^2\text{-Ph–C}\equiv\text{C–Ph}\}$ (**2d**) as the catalyst, only low conversions of diphenylacetylene (26%, entry 11) were achieved, and characteristic signals consistent with 9,10-diphenylphenanthrene could be observed by ^{1}H NMR spectroscopy. The formation of this product has been previously reported when treating $(L)_nNi(2,2'\text{-biphenyl})$ [where L = $(Et_3P)_2$ or $^iPr_2PCH_2CH_2P^iPr_2$] complexes with diphenylacetylene,[31,56] and this could be upgraded to catalytic regimes when using biphenylene and diphenylacetylene in the presence of O_2.[31] Compound **2d** was also found to catalyse the insertion of diphenylacetylene into the strained C–C bond of biphenylene (Scheme 4), however this process is slow (10 mol%, 40 hours, 80 °C), particularly when compared to a $Ni(NHC)_2$ catalyst reported by Radius (2 mol%, 30 min, 80 °C).[30] Attempts to spectroscopically identify or isolate possible intermediates for the [2 + 2 + 2] cyclotrimerisation of diphenylacetylene, or insertion of diphenylacetylene into biphenylene failed.

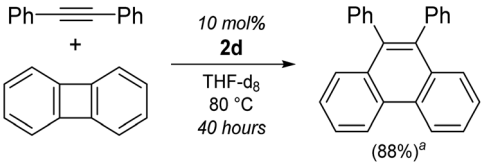

Scheme 4 Insertion of diphenylacetylene into biphenylene using catalytic $Li_2(THF)_4(2,2'\text{-biphenyl})Ni\{\mu_2\text{-}\eta^2\text{:}\eta^2\text{-Ph–C}\equiv\text{C–Ph}\}$ (**2d**). [a] Spectroscopic yield of 9,10-diphenylphenanthrene determined against hexamethylbenzene as an internal standard.

Table 2 Cyclotrimerisation of diphenylacetylene using different nickel catalysts

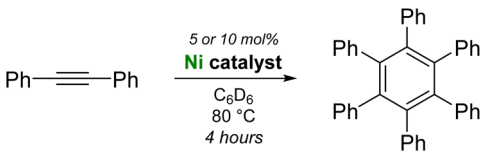

Entry	Catalyst	Conversion[a] (%)
1	5% $[(COD)Ni]_2\{PhC\equiv CPh\}$	38
2	5% Ni_2COT_2	41
3	5% $Li_4(Et_2O)_4Ph_4Ni_2\{PhC\equiv CPh\}$, **1a**	74
4	5% $Na_4(THF)_6Ph_4Ni_2\{PhC\equiv CPh\}$, **1b**	73
5	5% $K_4(THF)_4Ph_4Ni_2\{PhC\equiv CPh\}$, **1c**	78[b]
6	5% $Li_4(Et_2O)_4(4\text{-}^t\text{Bu-}C_6H_4)_4Ni_2\{PhC\equiv CPh\}$, **1d**	85
7	5% $Li_4(Et_2O)_4(C\equiv CPh)_4Ni_2\{PhC\equiv CPh\}$, **V**	Trace
8	10% $Li_2(THF)_2(o\text{-Tol})_2Ni\{PhC\equiv CPh\}$, **2a**	>95
9	10% $Li_2(Et_2O)_2(1\text{-Naph})_2Ni\{PhC\equiv CPh\}$, **2b**	74
10	10% $Li_2(Et_2O)_2(2,6\text{-}Me_2\text{-}C_6H_3)_2Ni\{PhC\equiv CPh\}$, **2c**	>95
11	10% $Li_2(THF)_4(2,2'\text{-biphenyl})Ni\{PhC\equiv CPh\}$, **2d**	26[b]

[a] Spectroscopic conversion of diphenylacetylene monitored using hexamethylbenzene as an internal standard. [b] Reaction performed in THF-d_8.

Conclusions

In conclusion, we have demonstrated that diphenylacetylene is a versatile π-accepting ligand which enables the facile synthesis of a family of mono- and dinickelate complexes. This methodology is compatible with a range of aryl substituents and alkali-metals, allowing the first homologous alkali-metal (AM = Li, Na, K) nickelate series to be isolated and characterised. These well-defined heterobimetallic complexes provide a rich platform to investigate and compare the unique spectroscopic and structural features of alkali-metal nickelates and help us understand the design principles required to access new low-valent nickelates. In addition, the catalytic ability of

the diphenylacetylene stabilised alkali-metal nickelates has also been investigated for the [2 + 2 + 2] cyclotrimerisation of diphenylacetylene, or the insertion of diphenylacetylene into biphenylene. Overall, these studies advance our understanding on how highly reactive mixed alkali-metal/Ni(0) complexes can be stabilised and structurally defined, as well as expanding on their potential to mediate catalytic C–C bond forming processes.

Conflicts of interest

There are no conflicts to declare.

Acknowledgements

The X-ray crystal structure determination service unit at Universität Bern is acknowledged for measuring, solving, refining, and summarising all new structures. The Synergy diffractometer used for X-ray single crystal structure determination was partially funded by the Swiss National Science Foundation (SNSF) within the R'Equip programme (project number 206021_177033). We thank Dr Ilche Gjuroski (NMR) and Andrea Bill (CHN) for analytical services, and Universität Bern and the SNSF (project grant 188573 to EH) for generous sponsorship of this research.

Notes and references

1 K. Fischer, K. Jonas, P. Misbach, R. Stabba and G. Wilke, *Angew. Chem., Int. Ed. Engl.*, 1973, **12**, 943–1026.
2 V. K. Jonas and C. Krüger, *Angew. Chem., Int. Ed. Engl.*, 1980, **19**, 520–537.
3 K. Fischer, K. Jonas and G. Wilke, *Angew. Chem., Int. Ed. Engl.*, 1973, **12**, 565–566.
4 K. Jonas, P. Heimbach and G. Wilke, *Angew. Chem., Int. Ed. Engl.*, 1968, **7**, 949–950.
5 V. B. Bogdanović, M. Kröner and G. Wilke, *Justus Liebigs Ann. Chem.*, 1966, **669**, 1–23.
6 K. Jonas, K. R. Pörschke, C. Krüger and Y. H. Tsay, *Angew. Chem., Int. Ed. Engl.*, 1976, **15**, 621–922.
7 K. Jonas, *Angew. Chem., Int. Ed. Engl.*, 1976, **15**, 47.
8 D. J. Brauer, C. Krüger, P. J. Roberts and Y. H. Tsay, *Angew. Chem., Int. Ed. Engl.*, 1976, **15**, 48–49.
9 K. R. Pörschke, K. Jonas, G. Wilke, R. Benn, R. Mynott and R. Goddard, *Chem. Ber.*, 1985, **118**, 275–297.
10 K. R. Pörschke, K. Jonas and G. Wilke, *Chem. Ber.*, 1988, **121**, 1913–1919.
11 W. Kaschube, K. R. Pörschke, K. Angermund, C. Krüger and G. Wilke, *Chem. Ber.*, 1988, **121**, 1921–1929.
12 K. R. Pörschke, W. Kleimann, Y. H. Tsay, C. Krüger and G. Wilke, *Chem. Ber.*, 1990, **123**, 1267–1273.
13 K. R. Pörschke and G. Wilke, *Chem. Ber.*, 1985, **118**, 313–322.
14 K. R. Pörschke and G. Wilke, *J. Organomet. Chem.*, 1988, **349**, 257–261.
15 K. R. Pörschke and G. Wilke, *J. Organomet. Chem.*, 1988, **358**, 519–524.
16 C. Krüger and Y. H. Tsay, *Angew. Chem., Int. Ed. Engl.*, 1973, **12**, 998–999.
17 K. Jonas, *Angew. Chem., Int. Ed. Engl.*, 1973, **12**, 997–998.
18 K. Jonas, D. J. Brauer, C. Krüger, P. J. Roberts and Y. H. Tsay, *J. Am. Chem. Soc.*, 1976, **98**, 74–81.
19 A. M. Borys and E. Hevia, *Angew. Chem., Int. Ed.*, 2021, **60**, 24659–24667.
20 A. M. Borys, L. A. Malaspina, S. Grabowsky and E. Hevia, *Angew. Chem., Int. Ed.*, 2022, **61**, e202209797.
21 S. Z. Tasker, E. A. Standley and T. F. Jamison, *Nature*, 2014, **509**, 299–309.
22 H. Ogawa, H. Minami, T. Ozaki, S. Komagawa, C. Wang and M. Uchiyama, *Chem. – Eur. J.*, 2015, **21**, 13904–13908.
23 K. Kojima, Z. K. Yang, C. Wang and M. Uchiyama, *Chem. Pharm. Bull.*, 2017, **65**, 862–868.
24 A. M. Borys and E. Hevia, *Synthesis*, 2022, 2976–2990.
25 R. J. Somerville, A. M. Borys, M. Perez-Jimenez, A. Nova, D. Balcells, L. A. Malaspina, S. Grabowsky, E. Carmona, E. Hevia and J. Campos, *Chem. Sci.*, 2022, **13**, 5268–5276.
26 E. L. Muetterties, W. R. Pretzer, M. G. Thomas, B. F. Beier, D. L. Thorn, V. W. Day and A. B. Anderson, *J. Am. Chem. Soc.*, 1978, **100**, 2090–2096.
27 V. W. Day, S. S. Abdel-Meguid, S. Dabestani, M. G. Thomas, W. R. Pretzer and E. L. Muetterties, *J. Am. Chem. Soc.*, 1976, **98**, 8289–8291.
28 J. Wei, W. X. Zhang and Z. Xi, *Angew. Chem., Int. Ed.*, 2015, **54**, 5999–6002.
29 A. Enachi, D. Baabe, M. K. Zaretzke, P. Schweyen, M. Freytag, J. Raeder and M. D. Walter, *Chem. Commun.*, 2018, **54**, 13798–13801.
30 T. Schaub and U. Radius, *Chem. – Eur. J.*, 2005, **11**, 5024–5030.
31 B. L. Edelbach, R. J. Lachicotte and W. D. Jones, *Organometallics*, 1999, **18**, 4660–4668.
32 H. J. Reich, D. P. Green, M. A. Medina, W. S. Goldenberg, B. Ö. Gudmundsson, R. R. Dykstra and N. H. Phillips, *J. Am. Chem. Soc.*, 1998, **120**, 7201–7210.
33 A. M. Borys and E. Hevia, *Organometallics*, 2021, **40**, 442–447.
34 B. Cordero, A. E. Platero-prats, M. Rev, J. Echeverr, E. Cremades and F. Barrag, *Dalton Trans.*, 2008, 2832–2838.
35 C. A. Murillo, *Multiple Bonds Between Metal Atoms*, Springer-Verlag, New York, 2005, pp. 633–667.
36 M. Bolte, *CSD Commun.*, 2011, DOI: **10.5517/ccxmqs0**.
37 W. Uhl, E. Er and M. Matar, *Z. Anorg. Allg. Chem.*, 2006, **632**, 1011–1017.
38 D. T. Carey, F. S. Mair, R. G. Pritchard, J. E. Warren and R. J. Woods, *Eur. J. Inorg. Chem.*, 2003, 3464–3471.
39 D. Walther, M. Stollenz and H. Görls, *Organometallics*, 2001, **20**, 4221–4229.
40 S. Saito and Y. Yamamoto, *Chem. Rev.*, 2000, **100**, 2901–2915.

41 S. Kotha, E. Brahmachary and K. Lahiri, *Eur. J. Org. Chem.*, 2005, 4741–4767.
42 P. R. Chopade and J. Louie, *Adv. Synth. Catal.*, 2006, **348**, 2307–2327.
43 W. Reppe, O. Schlichting, K. Klager and T. Toepel, *Justus Liebigs Ann. Chem.*, 1948, **560**, 1–92.
44 W. Reppe and W. J. Schweckendiek, *Justus Liebigs Ann. Chem.*, 1948, **560**, 104–116.
45 B. F. Straub and C. Gollub, *Chem. – Eur. J.*, 2004, **10**, 3081–3090.
46 J. Montgomery, *Angew. Chem., Int. Ed.*, 2004, **43**, 3890–3908.
47 A. Thakur and J. Louie, *Acc. Chem. Res.*, 2015, **48**, 2354–2365.
48 S. K. Rodrigo, I. V. Powell, M. G. Coleman, J. A. Krause and H. Guan, *Org. Biomol. Chem.*, 2013, **11**, 7653–7657.
49 S. Pal and C. Uyeda, *J. Am. Chem. Soc.*, 2015, **137**, 8042–8045.
50 D. J. Brauer and C. Krüger, *J. Organomet. Chem.*, 1976, **122**, 265–273.
51 M. Fairley, L. Davin, A. Hernán-Gómez, J. García-Álvarez, C. T. O'Hara and E. Hevia, *Chem. Sci.*, 2019, **10**, 5821–5831.
52 L. Davin, A. Hernán-Gómez, C. McLaughlin, A. R. Kennedy, R. McLellan and E. Hevia, *Dalton Trans.*, 2019, **48**, 8122–8130.
53 M. De Tullio, A. M. Borys, A. Hernán-Gómez, A. R. Kennedy and E. Hevia, *Chem Catal.*, 2021, **1**, 1308–1321.
54 T. X. Gentner, A. R. Kennedy, E. Hevia and R. E. Mulvey, *ChemCatChem*, 2021, **13**, 2371–2378.
55 A. W. J. Platten, A. M. Borys and E. Hevia, *ChemCatChem*, 2022, **14**, 2–7.
56 J. J. Eisch, A. M. Piotrowski, K. I. Han, C. Krüger and Y. H. Tsay, *Organometallics*, 1985, **4**, 224–231.